New Phytologist

Research

Flashy, decoupled, or declining? Single theories fail to explain the diversity of drought mortality signals in tree rings

Alicia Formanack[1], Kiona Ogle[1] and Drew Peltier[2]

[1]School of Informatics, Computing, and Cyber Systems, Northern Arizona University, Flagstaff, AZ 86011, USA; [2]School of Life Sciences, University of Nevada, Las Vegas, NV 89119, USA

Author for correspondence:
Alicia Formanack
Email: amf258@nau.edu

Received: *15 March 2025*
Accepted: *11 September 2025*

New Phytologist (2025) **248:** 2795–2808
doi: 10.1111/nph.70605

Key words: climate decoupling, climatic sensitivity, drought mortality, flashy growth, forest decline, tree growth, tree rings.

Summary

- Growth patterns recorded in tree rings may predict drought 'winners' and 'losers'. Past studies of drought-killed trees have produced conflicting evidence. Some show killed trees were highly responsive to climate, while others suggest killed trees were climate-insensitive or became less sensitive over time.
- We leveraged ring width data from 2934 drought-killed and -surviving trees of seven species to compute growth sensitivity to seasonal climate variables via a Bayesian mixed effects model. Aided by clustering analyses, we evaluated how species conformed to three alternative hypotheses (theories): relative to surviving trees, killed trees (H1) have 'flashy' climate responses, (H2) are 'decoupled' from climate, or (H3) have 'declining' sensitivity over time.
- Differences in growth patterns were not consistent across species or status (surviving/killed). Drought-killed subalpine fir and Engelmann spruce exhibited 'flashy' growth – higher sensitivity of growth to climate over time – compared with survivors. Drought-killed aspen, Scots pine, and Norway spruce showed stable, climate-insensitive growth compared with survivors, suggesting 'decoupling' from climate. Most species showed nonstationary sensitivities, but rather than declining, some sensitivities increased, even in surviving trees.
- Our flashy-decoupled-declining framework links predictions for future drought-induced mortality to potential mechanisms, enhancing ecological and physiological understanding of growth–climate patterns preceding drought mortality events.

Introduction

Forests play a dominant role in the terrestrial carbon cycle and are increasingly threatened by large-scale mortality events (Van Mantgem *et al.*, 2009; Allen *et al.*, 2015; Anderegg *et al.*, 2020). With rising temperatures and intensification of the water cycle (Swain *et al.*, 2025), droughts are affecting tree growth and mortality across all biomes (Allen *et al.*, 2010; Hammond *et al.*, 2022). In response to drought, tree species can exhibit various survival strategies that interact with climate variability, forest dynamics, and physiological traits (Baldi & La Porta, 2022). Identifying intra- and interspecific patterns in tree growth responses to drought is thus essential to understanding risks to future carbon storage (Chen *et al.*, 2012; Gazol *et al.*, 2018; DeSoto *et al.*, 2020; Zeng *et al.*, 2023). Moreover, understanding how tree growth responds to climate over time could point to intraspecific growth strategies that create drought 'winners' and 'losers' (Gazol *et al.*, 2023).

Tree rings provide temporally rich, annually resolved data on the relationship between tree growth and climate (Martinelli, 2004; Schöngart *et al.*, 2006; Tipton *et al.*, 2016) and have even shown early warning signs of mortality up to 20 yr preceding death (Cailleret *et al.*, 2019). Numerous studies of tree drought mortality have been conducted (Mäkinen *et al.*, 2001; Bigler *et al.*, 2004; Haavik *et al.*, 2011; Ireland *et al.*, 2014), yet our ability to predict drought-related mortality remains poor (Meir *et al.*, 2015; McDowell *et al.*, 2016). Furthermore, growth responses to climate (i.e. climate sensitivity) are influenced by many factors including physiological traits, microsite conditions, competition, and genetic variation (Gessler *et al.*, 2017; Choat *et al.*, 2018; Trugman *et al.*, 2021). The study of drought-killed trees can therefore be useful to identify the diversity of drought-response strategies and to understand regionally specific patterns in climate sensitivity of dying trees (Cailleret *et al.*, 2019; DeSoto *et al.*, 2020).

We identified three competing concepts of how the likelihood of drought-induced mortality could be inferred from tree-ring time series. For some species, (1) highly variable growth–climate responses over time can be indicative of a higher potential for mortality (Ogle *et al.*, 2000; Cailleret *et al.*, 2017, 2019; Smith *et al.*, 2019). This 'flashy' growth response to climate may be a drought strategy focused on recovery instead of avoidance but could also reflect more 'acquisitive' traits (Wright *et al.*, 2010; Maracahipes *et al.*, 2018; Umaña *et al.*, 2023) that entail greater risk during drought events. By contrast, (2) both low climate sensitivity and low growth can indicate a higher probability of future mortality (Bigler *et al.*, 2006; Gillner *et al.*, 2013; DeSoto *et al.*, 2020). Often, such trees have radial growth that appears

'decoupled' from climate, showing small ring widths with very little variation (i.e. reduced sensitivity to climate variation). Several other studies describe tree and forest mortality in the context of (3) 'declining' growth, in which reductions in growth or climate sensitivity associated with an inciting event (e.g. a severe drought) can subsequently lead to eventual mortality (Minorsky, 2003; Voelker *et al.*, 2008; Amoroso *et al.*, 2017). In this scenario, declining trees never recover to predrought levels of growth or climate sensitivity and slowly die (Bigler *et al.*, 2007; Cailleret *et al.*, 2017; DeSoto *et al.*, 2020). It remains unclear whether any of these growth patterns are universal, as past studies employed different approaches, or whether tree growth in dying trees proceeds differently in different species and regions of the world.

Tree growth strategies may represent trade-offs that influence tree responses to drought stress, leading to either survival or mortality (Willi & Van Buskirk, 2022). Thus, improved characterization and understanding of tree growth patterns are essential to identifying potential winners and losers in the face of climate change. For example, radial tree growth with 'flashy' climate sensitivity could be indicative of trees prioritizing growth over repair, possibly leading to early death if drought return intervals are short (Anderegg *et al.*, 2012). Such strategies may also reflect other life-history trade-offs, in which, for example, we might expect primary successional species that prioritize growth to quickly reach dominant canopy status to do so at the expense of biotic defense (Crouch *et al.*, 2021). Tree growth that is less temporally variable, appearing 'decoupled' from climate, could be a strategy focused on continuous allocation to repair, defense, or maintenance at the cost of low growth (Anderegg *et al.*, 2015; Peltier *et al.*, 2016; Huang *et al.*, 2021; Leifsson *et al.*, 2023), or an indication of competition-stress (Ford *et al.*, 2017; Luo *et al.*, 2020). Importantly, more frequent regional droughts and rising temperatures (Williams *et al.*, 2022) are likely leading to gradual changes in growth–climate sensitivity over time (Peltier & Ogle, 2020; Wilmking *et al.*, 2020), which is likely to be species-dependent.

We evaluated growth–climate relationships of drought-surviving trees and drought-killed trees using tree-ring data from seven species (five gymnosperms and two angiosperms) in the United States and western Europe. We sought to understand how growth–climate responses (i.e. climate 'sensitivities') differed between drought-killed and drought-surviving trees of the same species. We developed a Bayesian hierarchical model that estimated the effects of climate on ring width, including lagged climate effects ('memory'; Ogle *et al.*, 2015). We computed indices of ring width sensitivity to different seasonal climate variables and performed clustering of those sensitivity indices, allowing us to evaluate three hypotheses related to the growth patterns of drought-killed trees relative to drought-surviving trees, which we will refer to throughout as (H1) flashy, (H2) decoupling, and (H3) declining. We hypothesized that (H1) dying trees were more sensitive to climate before death, with higher variation in growth than surviving trees of the same species, reflecting a 'flashy', more acquisitive growth strategy. Alternatively, (H2) dying trees were less sensitive to seasonal climate ('decoupled'), reflecting a more conservative growth strategy. As a third alternative, (H3) dying trees were 'declining' (i.e. gradual weakening of growth–climate sensitivities over time), demonstrating their inability to recover from damage incurred by past stress. Our results highlight the complexity and diversity of tree growth responses to climate stress within and among species, and that these responses likely depend upon site history and species traits (e.g. acquisitive vs conservative) that influence their physiological behavior and lead to differing drought responses.

Materials and Methods

Study area and species

We used a subset of records from a previously compiled dataset comprising 58 published and unpublished studies of tree-ring widths and mortality (Cailleret *et al.*, 2017). At each site, drought-surviving and drought-killed trees of the same species were identified and cored; tree cores were cross-dated and annual ring widths measured using standard dendrochronology methods (Stokes, 1996). From this dataset, we extracted 133 sites (23 species) in which 'drought' was reported as the predominant cause of tree mortality. We further subset the data, selecting species with at least 100 trees (surviving and killed trees combined), producing a dataset with 93 sites consisting of 12 different species. We incorporated data for another species (*Populus tremuloides*, quaking aspen) representing 18 sites in the western United States (Ireland *et al.*, 2014). Some species were excluded following preliminary analyses due to poor model mixing and convergence issues, likely resulting from comparatively small sample sizes or nonsignificant climate effects due to the use of relatively coarse climate data (see 'Climate data' in the Materials and Methods section). The final datasets thus consisted of seven species (Table 1) that are widely studied, commercially and culturally important, and have distributions spanning North America and Europe (Fig. 1). These species represent both conifers and broadleaf species: *Pinus sylvestris* L. (Scots pine), *Abies alba* Mill. (silver fir), *Quercus rubra* L. (red oak), *Picea engelmannii* Parry ex Engelm. (Engelmann spruce), *Picea abies* (L.) Karst. (Norway spruce), *P. tremuloides* Michx. (quaking aspen), and *Abies lasiocarpa* (Hook.) Nutt. (subalpine fir).

Climate data

Monthly climate data (mean temperature and total precipitation) were obtained from the Climatic Research Unit (CRU) gridded dataset (0.5° resolution) for the 1901–2017 period (Harris *et al.*, 2020). Although it is likely that climate data at such coarse resolution can fail to capture microclimate conditions that trees experience (Ford *et al.*, 2013), CRU gridded data met our temporal and spatial requirements needed to match our annual tree-ring data. We anticipated that (1) growth sensitivities to climate (e.g. temperature and precipitation) depend on the seasonality of climate, in which effects may differ between cold (e.g. winter) and warm (e.g. summer) seasons, and (2) changes

Table 1 Summary of data, including number (N) of trees, by status (drought-surviving = live; drought-killed = dead), and number of sites.

Species	Live trees (N)	Dead trees (N)	Sites (N)	MAT (°C)	Summer MT (°C)	Winter MT (°C)	MAP (mm)	Summer MP (mm)	Winter MP (mm)	Data source(s)
Abies alba (silver fir)	290	128	11	9.5 (±0.7)	14.9 (±0.9)	4.2 (±0.8)	1044 (±151)	518 (±97)	525 (±110)	Bigler *et al.* (2004), Cailleret *et al.* (2014), Linares and Camarero (2012)
Abies lasiocarpa (subalpine fir)	87	70	13	1.6 (±0.7)	8.8 (±0.8)	−5.7 (±1.0)	408 (±65)	237 (±50)	171 (±38)	Bigler *et al.* (2007)
Picea abies (Norway spruce)	237	151	18	3.5 (±1.0)	11.3 (±0.8)	−4.4 (±1.6)	613 (±68)	363 (±57)	250 (±32)	Aakala *et al.* (2011), Mäkinen *et al.* (2001)
Picea engelmannii (Engelmann spruce)	93	50	14	1.6 (±0.7)	8.8 (±0.8)	−5.7 (±1.0)	408 (±65)	237 (±50)	171 (±38)	Bigler *et al.* (2007)
Pinus sylvestris (Scots pine)	363	245	12	7.0 (±0.7)	12.3 (±0.8)	1.7 (±0.8)	1051 (±102)	564 (±69)	488 (±70)	Bigler *et al.* (2006), Gea-Izquierdo *et al.* (2014), Heres *et al.* (2012), Sangüesa-Barreda *et al.* (2013)
Populus tremuloides (quaking aspen)	197	210	18	8.5 (±0.7)	14.9 (±0.7)	2.0 (±0.9)	512 (±118)	260 (±67)	252 (±98)	Ireland *et al.* (2014)
Quercus rubra (red oak)	684	129	7	15.0 (±0.7)	22.2 (±0.7)	7.7 (±1.0)	1170 (±197)	668 (±128)	502 (±123)	Haavik *et al.* (2011)

Species-level climate summaries are provided as mean annual temperature (MAT), mean annual precipitation (MAP), mean temperature (MT), and mean precipitation (MP) for each season (summer/winter). Climate summaries were averaged across sites for each species in the study, given as mean (±1 SE). The data source(s) include the original studies responsible for procuring the tree-ring data used in this study.

Fig. 1 Maps of sites located across the (a) United States and (b) Europe. The colored polygons represent the native ranges of each study species, and the points of the same color indicate the sites where each species was sampled. (a) In the United States, the species include aspen, subalpine fir, Engelmann spruce, and northern red oak; (b) in Europe, they include Norway spruce, silver fir, and Scots pine.

(trends) in such sensitivities might also depend on season. Thus, we aggregated monthly climate data into 'seasons' (i.e. winter and summer). Summer represents the current year's growing season and was defined as the months with higher-than-average monthly temperatures, in which the average (mean) temperature was computed across all months over the period 1905–2016. The winter season includes months with lower-than-average monthly temperatures, when trees are likely dormant. Therefore, the winter season begins in the year preceding the growing season, as the effects of winter do not impact tree radial growth until the subsequent growing season. Winter and summer season definitions can vary by site; for instance, a particular site might define winter as October to March and summer as April to September, whereas another site might define winter as September to February and summer as March to August.

Model description and implementation

Since studies have revealed that the effects of climate on tree growth (ring widths) can last up to 4 years after an extreme climate event (Anderegg *et al.*, 2015), we implemented a variant of the Bayesian stochastic antecedent modeling (SAM) framework (Ogle *et al.*, 2015; Peltier *et al.*, 2018) to estimate the impact of current and past climate, up to 4 years before ring formation. Distinct from previous SAM variants applied to tree-ring data (e.g. Peltier *et al.*, 2018), we allowed the effects of temperature and precipitation to vary by season, thus allowing for the possibility of season-specific influences of a given climate covariate (e.g. temperature). Furthermore, to account for site-level climate variation and its effects on climate sensitivity, we chose to model climate sensitivities hierarchically. Therefore, we implemented a Bayesian hierarchical regression model for tree growth (i.e. ring width) vs seasonal climate (e.g. winter and summer precipitation and temperature) to explore variation in climate sensitivity between drought-killed and drought-surviving trees. Below, we describe the model structure, which we implemented separately for drought-killed and drought-surviving trees, for each species.

The hierarchical Bayesian model that we implemented is analogous to a mixed effects regression model. Within the Bayesian framework, we must specify (1) the likelihood of the data (response variable) based on an appropriate sampling distribution and (2) priors for unknown parameters in the model (i.e. regression coefficients, variance terms). The Bayesian procedure combines the likelihood and priors via Bayes theorem (Gelman *et al.*, 2014) to produce posterior estimates of all model parameters and any derived quantities (quantities that are functions of parameters and potentially data), thus explicitly quantifying uncertainty in these quantities. We thus began by defining the likelihood of log-transformed ring width, $RW = \log(r+1)$, where r is the original ring width (mm), and we add 1 to r since some cores had missing rings (i.e. $r = 0$). For each year y and core c, we assumed that $RW_{y,c}$ was normally distributed, with mean $\mu_{r,c}$ and variance σ^2:

$$RW_{y,c} \sim Normal\left(\mu_{y,c}, \sigma^2\right) \quad \text{Eqn 1}$$

The mean log-scale ring width, $\mu_{y,c}$, is regressed on tree age (*Age*) at the time of ring formation, the previous year's growth index ($RW_{y-1,c}$), and antecedent seasonal precipitation (P^{ant}), temperature (T^{ant}), and their interactions ($P^{ant} \times T^{ant}$). For simplicity, let X_1, X_2, X_3, and X_4 denote winter P^{ant}, summer P^{ant}, winter T^{ant}, and summer T^{ant}, respectively. The mean model is as follows:

$$\mu_{y,c} = \alpha_{1,c} + \alpha_{2,c} \cdot Age_{y,c} + \alpha_{3,c} \cdot RW_{y-1,c} + \sum_{j=1}^{4} \beta_{j,s(c)} \cdot X_{j,y,s(c)} + \sum_{k=j+1}^{4} \sum_{j=1}^{3} \gamma_{j,k,s(c)} \cdot X_{j,y,s(c)} \cdot X_{k,y,s(c)} \quad \text{Eqn 2}$$

The intercept (α_1), age effect (α_2), and autoregressive effect (α_3) all vary at the level of core, c. The main effects ($\beta_1, \ldots, \beta_4$) of antecedent seasonal climate (X_j terms) all vary at the level of site, where $s(c)$ denotes site s associated with core c. Similarly, the six different two-way interaction effects ($\gamma_{1,2}, \ldots, \gamma_{3,4}$) associated with interactions between climate variables X_j and X_k also vary at the level of site, s. All two-way climate interactions were included to account for nonlinear effects of climate on tree growth (Lloyd *et al.*, 2013; Wilmking *et al.*, 2020). Age ($Age_{y,c}$) and prior growth ($RW_{y-1,c}$) were standardized at the core level such that both have a mean of zero and a standard deviation (SD) of 1. The antecedent climate covariates (X terms) are based on standardized seasonal climate data (will be discussed later).

The antecedent climate variables, P^{ant} and T^{ant} (or, more generally, X_1, X_2, X_3, and X_4), are calculated as the weighted averages of the yearly seasonal total precipitation or average temperature over the past 4 years up to and including the end of the concurrent growing season. For antecedent climate variable X_j, in year y at site s:

$$X_{j,y,s} = \sum_{t=0}^{4} w_{j,t} \cdot x_{j,y-t,s} \quad \text{Eqn 3}$$

Note that $x_{j,y,s}$ denotes the original, yearly, standardized seasonal climate variable, in which each climate variable was standardized by site within a given species using site-level means and SD. The importance weights, $w_{j,t}$, are unique to each climate variable for each species but assumed invariant across sites within a species; the weights were estimated for each year t into the past up to 4 years ago relative to year y for each variable X_j. Weights were constrained to sum to 1 across all lags ($t = 0$ (concurrent year), 1, 2, 3, 4) for a given variable and season, so they are interpreted as the relative importance of climate during a given 'lag' year and season for each climate variable.

To complete the model specification, we assigned standard, relatively noninformative priors to all parameters in the model. We assumed hierarchical priors for the core-level (i.e. α terms) and site-level parameters (e.g. β and γ terms) in Eqn (2), thus treating core and site as random effects. The core-level parameters (α terms) were assigned hierarchical normal priors that varied around site-level means. All site-level parameters (β and γ terms and site-level means for the α terms) were assigned hierarchical normal priors that varied around global means representing the species-status group effects (status = 'drought-killed' or 'surviving'), thus treating species-status group as fixed effects. Relatively noninformative (diffuse) normal priors were assigned to the global means, and wide uniform priors were assigned to all SD terms introduced by the hierarchical priors. A relatively noninformative Dirichlet prior was assigned to the yearly seasonal importance weights ($\boldsymbol{w}_j$ vectors, each length 5) in Eqn (3) to ensure that the weights sum to 1 and are constrained between 0 and 1. Diffuse normal priors, wide uniform priors, and relatively noninformative priors all minimize the influence of the prior on the posterior results, allowing the data and the likelihood to primarily govern the posterior estimates of the model parameters (Gelman *et al.*, 2014).

The model described by Eqns (1–3) was fit in JAGS 4.0.0 (Plummer, 2003) via the R (R Core Team, 2022) packages RJAGS (Plummer, 2008) and JAGSUI (Kellner, 2024) following standard

Markov chain Monte Carlo (MCMC) simulation methods. To explore mixing and convergence of sampled parameters (i.e. the MCMC sequences), we used the potential scale reduction factor (psrf) (Gelman & Rubin, 1992; Brooks & Gelman, 1998) via the autojags function in the JAGSUI package. Models were deemed to have converged if the psrf point estimates of all parameters were < 1.1. Posterior summary statistics were calculated for each quantity of interest, including the posterior mean, SD, and 95% central credible interval (CI) defined by the 2.5th and 97.5th percentiles. Parameters were considered significantly different between status categories if the CI for one status category (e.g. surviving trees) did not contain the posterior mean of the other category (i.e. drought-killed trees). Climate sensitivities were considered statistically significant when the CI associated with the relevant coefficient (i.e. β or γ terms) did not include zero.

Realized climate sensitivities

Given Eqn (2) includes two-way interactions among climate variables, we cannot interpret the main effects as climate sensitivities. Thus, we quantified the growth sensitivities to the different seasonal climate variables by calculating the partial first derivatives of the expected (mean) log-scale ring width, μ, with respect to each climate variable. This calculated quantity (a 'realized climate sensitivity') summarizes the sensitivity of ring widths to seasonal climate by accounting for the main and interactive effects of different antecedent climate variables. We computed these realized climate sensitivities (RS) at the species- and status-level across years and sites. For example, the time-varying RS of log-scale ring width to antecedent winter precipitation, $X_{1,j}$ in Eqn (1), is computed as:

$$RS_{l,y} = \frac{d\widehat{\mu}_y}{d\widehat{X}_{1,y}} = \widehat{\beta}_1 + \widehat{\gamma}_{1,2} \cdot \widehat{X}_{2,y} + \widehat{\gamma}_{1,3} \cdot \widehat{X}_{3,y} + \widehat{\gamma}_{1,4} \cdot \widehat{X}_{4,y}$$

Eqn 4

The '^' notation for expected log-scale ring width, $\widehat{\mu}$, and for the climate variables, $\widehat{X}_{j,y}$, indicates site-level estimates of these quantities for a given species and status group. Similarly, the $\widehat{\beta}$ and $\widehat{\gamma}$ terms denote the global-level climate effects that are representative of the focal species-status group. The RS for a focal climate variable (e.g. $\widehat{X}_{1,y}$) varies annually, conditional on other climatic conditions occurring during each year, as governed by the interaction effects, for example $\widehat{\gamma}_{1,2}$, $\widehat{\gamma}_{1,3}$, and $\widehat{\gamma}_{1,4}$ in Eqn (2). Note that the RS values describe the degree to which $\log(r+1)$, where r (ring width) is in units of mm, changes in response to one SD change in each climate variable, and thus, the RS values are comparable across species and status groups.

Then, the $RS_{j,y}$ values for each climate covariate X_j are used to assess mean climate sensitivity, variability in (SD) climate sensitivity, and climate sensitivity trends (i.e. changes in sensitivity over time). In particular, first we calculated the overall mean sensitivity (averaging RS across all years) for each climate variable's sensitivity index (i.e. for each RS_j, $j = 1, 2, 3, 4$ variables). Second, we summarized the temporal variation in each RS_j (for each covariate X_j) by calculating the SD of the yearly RS values. Third, we evaluated the temporal trend of the RS_j indices across years by regressing the RS values on year and using the slope coefficient from those regressions as an index of trend. Importantly, the Bayesian approach allows us to obtain posterior distributions for the time-varying RS values, in addition to aforementioned summaries (mean, SD, trends). In particular, we computed the temporally varying RS indices for each climate variable and species using 15 000 posterior samples (5000 samples per chain; 3 chains) of the parameters ($\widehat{\beta}$ and $\widehat{\gamma}$ terms). Next, we computed all three RS indices (mean, SD, and slope or trend) for each posterior sample of the RS_j time series; then, we computed posterior mean and 95% CI of these 15 000 mean, SD, and slopes to provide overall estimates of mean sensitivity, temporal variability in the climate sensitivities, and temporal trends in the climate sensitivities for each species and status group.

Hierarchical clustering of realized climate sensitivities

To evaluate differences in growth–climate responses among species and status groups, we performed hierarchical clustering using the mean, SD, and trend of the RS indices for all climate variables across all species-status combinations. After standardizing the RS values, we calculated the distance matrix and performed complete hierarchical clustering in R using the hclust function. This analysis produced a dendrogram for which we could evaluate grouping (clusters) of species and status groups. Each branch should support species-status combinations (leaves) that share similar growth–climate characteristics based on the RS indices. The arrangement of the branches reveals how similar the RS indices of the leaves are to each other. The height (or length) of the branches shows how similar (or different) the RS indices of the leaves are from one another, with greater height indicating larger differences.

Results

Model performance

The coefficient of determination (R^2) from regressions of observed vs predicted ring widths (r) spanned 0.68–0.93 (see Supporting Information Fig. S1, for drought-killed trees and see Fig. S2, for drought-surviving trees), indicating that the model fit the data well across all species and status groups. The highest R^2 occurred for surviving and killed subalpine fir and surviving Engelmann spruce ($R^2 = 0.93$) and the lowest for surviving aspen ($R^2 = 0.68$). The model tended to fit the ring width data better for drought-killed trees such that the R^2 for drought-killed trees was higher than the R^2 for surviving trees for most species, except Engelmann spruce and subalpine fir.

Summary of seasonal climate effects

Across species and status groups, *c.* 80% of the climate main effects were significant (i.e. 95% CI did not contain zero), and

nearly 70% of the climate two-way interactions were significant. Some of the main effects differed between drought-killed and drought-surviving trees within a given species, which we summarize here. For gymnosperms, the effect of summer precipitation on ring width differed significantly between surviving and dying trees of the same species (Fig. S3). Surviving Scots pine, subalpine fir, and Norway spruce are expected to grow more in response to increases in summer precipitation than their drought-killed counterparts. Conversely, drought-killed silver fir and Engelmann spruce trees are expected to grow more in response to summer precipitation relative to surviving trees. Surviving Engelmann spruce trees were the only group responding negatively to summer precipitation. Although the winter precipitation effect was significant for over half the species, Norway spruce and subalpine fir were the only two species for which the effects of winter precipitation differed by status, with drought-killed trees responding positively and surviving trees responding negatively to increases in winter precipitation (Fig. S3).

The summer temperature effect was significant across all species (Fig. S3). Silver fir, subalpine fir, surviving aspen, and red oak growth were enhanced by warmer summer temperatures. By contrast, Scots pine, Engelmann spruce, killed aspen, and Norway spruce responded negatively to warmer summer temperatures. Summer temperature effects differed in sign only for surviving and killed aspen. Summer temperature effects differed in magnitude, but not sign, for subalpine fir and Engelmann spruce and did not differ in magnitude between surviving and dying trees for silver fir, red oak, Scots pine, and Norway spruce. However, the effect of winter temperature differed significantly between surviving and dying angiosperms; surviving aspen and red oak trees produced narrower rings with increasing winter temperatures. By contrast, winter temperature was nonsignificant for drought-killed red oak, while the effect was less negative for dying aspen compared to surviving aspen.

While the main effects offer initial insight into potential climate sensitivities, they must be interpreted with caution in the presence of interacting climate effects. Thus, we focus on the realized sensitivities next (RS, see Eqn 4; Figs S1).

Single growth strategies fail to capture diverse climate mortality signals

RS often differed between drought-killed and drought-surviving trees (Figs S4–S10), but differences were not consistent across species; we highlight three examples. Drought-killed subalpine fir exhibited highly variable sensitivity to winter temperatures, illustrating 'flashy' growth responses compared with drought-surviving trees (Fig. 2a). Drought-killed Scots pine showed reduced sensitivity to summer precipitation and overall lower variation in that sensitivity compared with drought-surviving trees (Fig. 2b), providing an example of dying trees that are relatively 'decoupled' from climate variation. Drought-killed silver-fir showed 'declining' sensitivity to summer temperature, but so did surviving silver-fir (Fig. 2c). In short, we found evidence for each of the three hypotheses, with different species' responses to seasonal climate aligning with different hypotheses.

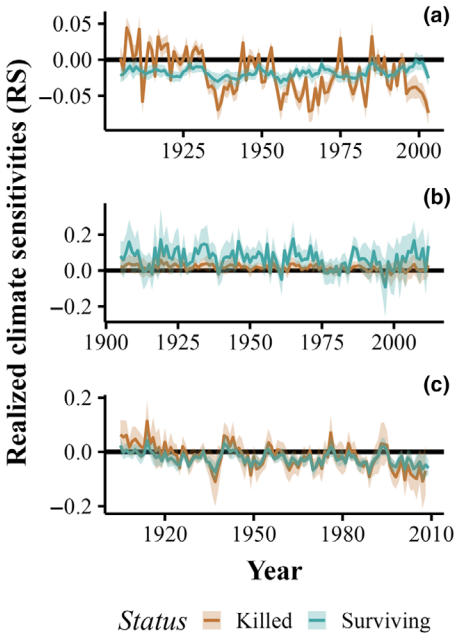

Fig. 2 Examples of realized climate sensitivities (RS) of log-scale ring width for different species. (a) Drought-killed subalpine fir trees are associated with high variation in the RS of growth to winter temperature, illustrating a 'flashy' growth strategy. (b) Drought-killed Scots pine trees show reduced sensitivity and lower variation in response to summer precipitation, an example of dying trees appearing 'decoupled' from climate. (c) Silver fir trees show declining sensitivity of growth to winter temperature over time regardless of status. Solid colored lines are the posterior means of the annual RS values; shaded regions denote the 95% central credible interval. The solid black horizontal line is the zero line.

Summarizing patterns in growth responses across RS indices, climate variables, species, and status groups, hierarchical clustering identified four relatively distinct groups (Fig. 3). Critically, all four groups contained dying trees of one species and surviving trees of another, indicating differences were not consistent across species or across status groups. The clustering algorithm placed drought-killed and drought-surviving trees in different groups for five species (Engelmann spruce, Norway spruce, Scots pine, subalpine fir, and aspen), indicating dying and surviving trees have different growth–climate sensitivities in these species (Fig. 3). Aspen is the only species for which drought-killed and drought-surviving trees were not only in different groups but they were also notably separated within the dendrogram. That is, drought-killed aspen were placed in Group 2 and surviving aspen in Group 3, indicating that the growth–climate relationships differed greatly among dying and living aspen (Fig. 3). Conversely, surviving and dying trees for two species (dead red oak and silver fir) were placed in the same group (4), suggesting that drought-killed and drought-surviving trees exhibited similar growth–climate characteristics for these two species (Fig. 3).

Evidence for flashy growth (H1)

We categorized growth–climate sensitivity as comparatively flashier when drought-killed (or drought-survived) trees had a higher

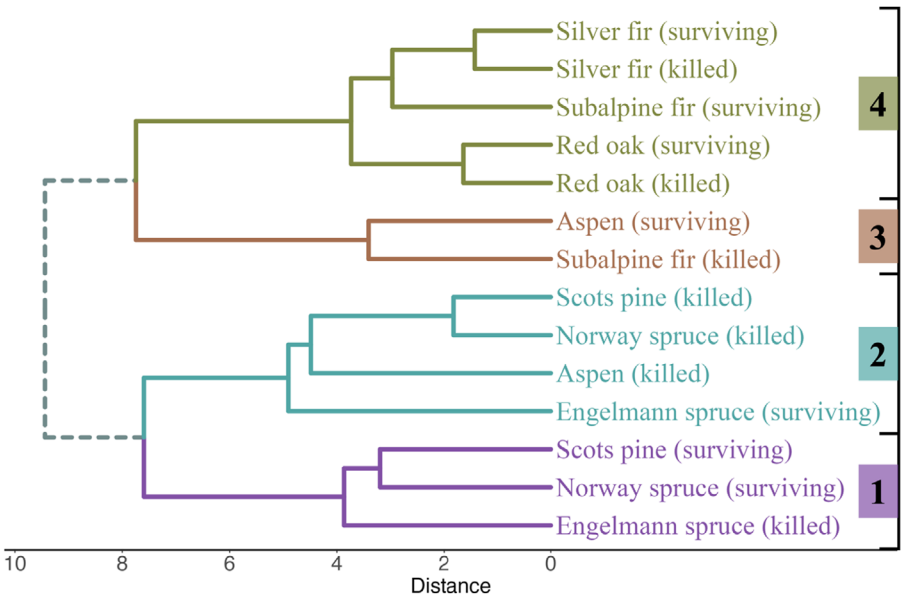

Fig. 3 Complete hierarchical clustering dendrogram using the mean, SD, and trend of the four seasonal realized climate sensitivities (RS). The cluster dendrogram shows four distinct groups of species/status combinations (leaves) that share similar growth–climate characteristics. The arrangement of the branches reveals how similar the RS of the leaves are to each other. The distance (length) of the branches (horizontal lines) shows how similar or different the RS of leaves are from one another, with greater height indicating larger differences.

RS mean and/or higher SD when compared to drought-surviving (or drought-killed) trees of the same species. Surviving Norway spruce and Scots pine, along with dying Engelmann spruce (Fig. 3; Group 1), had a high mean RS to summer precipitation; that is, increases in summer precipitation led to comparatively larger increases in ring width (Fig. 4b–d) across all three species in this group. Dying Engelmann spruce trees were almost twice as sensitive to summer precipitation relative to surviving trees (Fig. 4b), consistent with H1. The dendrogram branching structure in Group 1 (Fig. 3) suggests a subgroup consisting of surviving Norway spruce and Scots pine, which share high variability (high RS SD) in the effects of winter temperature and precipitation over time (Fig. 4g,h). Group 3 (Fig. 3) is the smallest group, consisting of dying subalpine fir and surviving aspen, which share high variability in the (negative) effects of winter temperature (Fig. 5a,d,e,h). The SD of RS to winter temperature for dying subalpine fir is 1.3 times higher than for surviving subalpine fir (Fig. 5h), consistent with H1. Surviving aspen shared this flashy response to winter temperature, compared with drought-killed aspen, with surviving aspen being 1.8 times more sensitive to winter temperature (Fig. 5a).

Evidence for decoupling (H2)

Ring widths in drought-surviving Engelmann spruce and in drought-killed Norway spruce and Scots pine (Fig. 3; group 2) are relatively insensitive to ('decoupled' from) summer precipitation (Fig. 4b–d,f–h). Their growth is only one-fifth as sensitive to summer precipitation as their drought-killed (Engelmann spruce) or surviving (Norway spruce and Scots pine) counterparts, supporting H2. The length of the dendrogram terminal branches within Group 2 (Fig. 3) suggests that dying Norway spruce and Scots pine have very similar growth characteristics, forming a subgroup of two. In addition to decoupling from summer precipitation, dying Norway spruce and Scots pine show little to no (positive) sensitivity to winter temperature, with very low variability (low SD) in the effects of winter temperature over time (Fig. 4c,d,g,h). Both drought-killed and drought-surviving silver fir, a subset of Group 4 (Fig. 3), appear decoupled from winter precipitation (Fig. 5c).

Drought-killed aspen showed five times less variation in growth due to the (negative) effects of winter temperature, compared with surviving aspen (Fig. 4a,e). Drought-killed aspen showing very low variability (low SD) in the effects of winter temperature over time supports H2 (Fig. 4e). Furthermore, drought-killed aspen were moderately less sensitive to and had less variation in response to summer temperature, and growth responses to summer temperature notably differed by status. Increasing summer temperature had the effect of reducing growth in drought-killed aspen but increasing growth in surviving aspen (Figs 4a, 5a).

Evidence for decline (H3)

The dendrogram (Fig. 3) shows that within Group 4, the branching patterns indicate that surviving and dying trees cluster closely together within two species (i.e. silver fir and red oak), implying that they share similar growth–climate relationships regardless of their status. Notably, surviving subalpine fir clusters more closely with both surviving and dying silver fir than with red oak, suggesting greater similarity in growth response between subalpine and silver fir than between subalpine fir and red oak. Surviving and dying red oak exhibit similar negative sensitivity to winter precipitation and positive sensitivity to summer precipitation (Fig. 5b). However, negative trends in summer temperature sensitivity and positive trends in winter precipitation sensitivity suggest declining sensitivities (Fig. 5j). Surviving and dying silver fir and surviving subalpine fir show declining sensitivity to summer temperature (Fig. 5k,l), as the positive effects of temperature diminished over time. Surviving Scots pine, surviving Norway

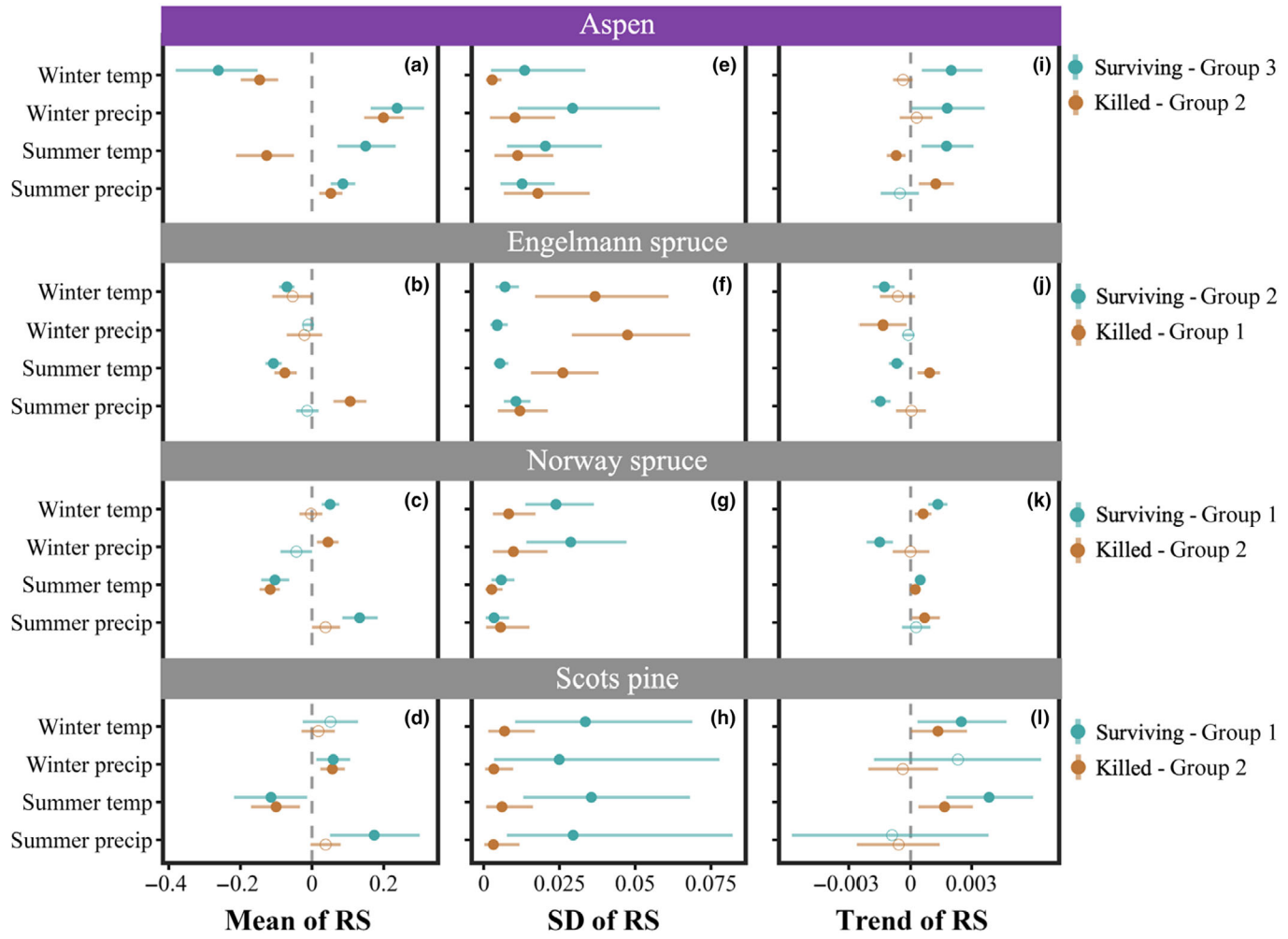

Fig. 4 Summary statistics of seasonal realized climate sensitivities (RS) for aspen, Engelmann spruce, Norway spruce, and Scots pine (Dendogram groups 1 and 2; Fig. 3). Summary statistics include posterior means and 95% central credible intervals (CIs) for the mean (a–d), SD (e–h), and temporal trend (i–l) in the annual RS values, faceted by species and colored by status. Filled symbols denote mean, SD, and trends that are significantly different from zero, and unfilled symbols represent those with 95% CI that cross zero (the gray vertical dashed line).

spruce, and dying Engelmann spruce (Fig. 3; Group 1) show negative sensitivity to summer temperature coupled with a positive trend (Fig. 4j–l), which implies decreasing sensitivity over time. Interestingly, drought-killed subalpine fir shows declining climate sensitivity to most climate variables, except for winter temperature, which shows an increasingly negative trend in sensitivity; thus, sensitivity to winter temperature has been increasing over time (Fig. 5d,l).

Geographical differences in trends

Although trends in growth–climate sensitivities (RS indices) were detected in multiple species, often these trends were not significantly different between surviving and dying trees of the same species. However, there were more significant differences in the trend of climate effects for surviving and dying trees in the arid southwestern United States. For example, drought-killed and surviving subalpine fir and Engelmann spruce trees had significantly different trends for all four seasonal climate variables. The average trend of RS to winter temperature, summer temperature, and summer precipitation differed significantly between drought-killed and surviving aspen trees. Additionally, subalpine fir, Engelmann spruce, and aspen all have at least one RS trend that differs in sign (i.e. positive/negative) between surviving and dying trees. Dying aspen show a negative trend in RS to summer temperature, indicating an exacerbating negative effect of summer temperature, in contrast to the enhanced positive effects of summer temperature for surviving aspen. Interestingly, dying Engelmann spruce have a positive trend of RS to summer temperature, indicating that the detrimental effects of summer temperature have been diminishing over time, whereas surviving trees show the opposite (a negative RS trend).

Discussion

Our study explored three hypotheses related to mechanisms underlying growth–climate responses of drought-killed trees relative to those that survive. Relative to surviving trees, drought-

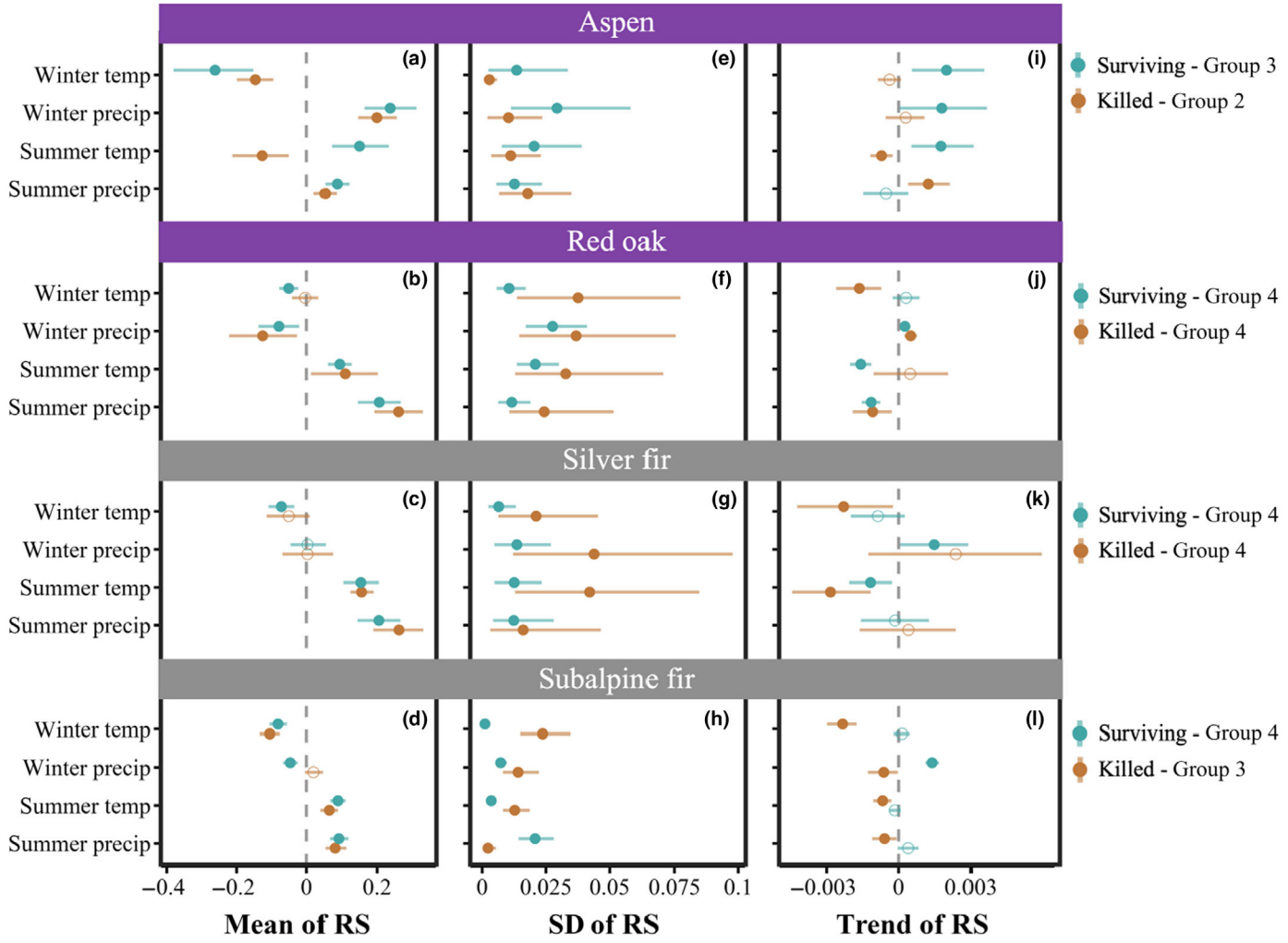

Fig. 5 Summary statistics of seasonal realized climate sensitivities (RS) for aspen, red oak, silver fir, and subalpine fir (Dendrogram groups 3 and 4; Fig. 3). Summary statistics include posterior means and 95% central credible intervals (CIs) for the mean (a–d), SD (e–h), and temporal trend (i–l) in the annual RS values, faceted by species and colored by status. Filled symbols denote mean, SD, and trends that are significantly different from zero, and unfilled symbols represent those with 95% CI that cross zero (the gray vertical dashed line).

killed trees either demonstrated highly variable growth–climate responses over time (flashy), low climate sensitivity, or low growth–climate variability (decoupled), or reductions in climate sensitivity over time (declining). No single hypothesis could describe the growth–climate patterns of drought-killed trees, as dying trees exhibited varied growth patterns across species. Drought-killed subalpine fir and Engelmann spruce exhibited 'flashy' growth in response to seasonal climate compared with conspecific trees that survived, supporting H1. Conversely, drought-killed Scots pine, Norway spruce, and aspen showed more stable, less climate-sensitive growth than survivors, reflecting 'decoupling' from climate, supporting H2. Moreover, silver fir and red oak had similar responses to climate across drought-surviving and drought-killed trees. Evidence of declining temperature and precipitation sensitivity was detected for surviving and dying silver fir and red oak, supporting H3. Drought-killed trees of many species also showed evidence of a decline in climate sensitivities for at least one seasonal climate variable. Interestingly, drought-killed trees of some species had positive trends in their climate sensitivities, the opposite of H3, indicating that these trees became more tightly coupled to climate over time. These differences may be explained by species traits, forest types, and region, where, for example, the time and severity of droughts have been very different between the United States and Europe. Integrating these multiple hypotheses together into a single framework provides an opportunity to understand the varied drivers of drought mortality across species and regions.

Flashy growth (H1) is a risky, resource-acquisitive strategy

In this study, Engelmann spruce and subalpine fir trees were generally sampled near the southern edge of their ranges, in which the risks and intensity of drought are likely the strongest (Sánchez-Salguero *et al.*, 2017; Anderegg *et al.*, 2019). For these

high-elevation sites, dying subalpine fir and Engelmann spruce showed high variation in growth sensitivity to winter temperature and precipitation. Bigler *et al.* (2007) showed that early-season droughts from 1978 to 2002 were more detrimental to subalpine fir and Engelmann spruce growth than late-season droughts, likely due to heavy reliance on winter snowpack for growing season soil moisture. Warming winters can cause early snowmelt and runoff, leaving less water available for bud burst and growth early in the growing season. Their highly sensitive and variable (flashy) growth strategy might be beneficial if trees are able to quickly recover lost sapwood, leaf area, or fine roots after experiencing drought (Tomasella *et al.*, 2017; Hesse *et al.*, 2023). However, frequent and prolonged droughts may increase the risk of hydraulic failure (Li *et al.*, 2020).

Moreover, growth–climate responses that are highly flashy could lead to structural overshoot (Zhang *et al.*, 2021), potentially making trees more vulnerable to drought impacts such as mortality. An increase in biomass under favorable conditions due to flashy growth responses may be challenging to sustain during drought conditions, potentially resulting in cavitation or shedding of branches and needles, which causes significant interannual variability in growth (Nadal-Sala *et al.*, 2021). Surviving subalpine fir and Engelmann spruce trees displayed a more conservative strategy; these trees likely prioritized more energy-intensive carbon tasks, such as repair and defense, over rapid growth. While this conservative strategy may result in lower growth, allocation of carbon toward defense rather than growth could also reduce the risk of insect or pathogen attack, particularly since drought conditions often coincide with biotic pressures (Ogle *et al.*, 2000; Kolb *et al.*, 2019; Brienen *et al.*, 2020).

Decoupling (H2) suggests persistent hydraulic failure and carbon starvation

Unlike Engelmann spruce and subalpine fir, drought-killed aspen, Norway spruce, and Scots pine trees exhibited a lower sensitivity to climate relative to surviving trees. This pattern supports H2 and suggests a struggle to meet needs for even minimal growth (McDowell *et al.*, 2022). Dying aspen were affected by multiyear droughts from 2000 to 2008, coinciding with the megadrought spanning 2000 to 2018 (Ireland *et al.*, 2014; Williams *et al.*, 2020). Consistent with previous aspen drought mortality research, high summer temperatures are especially detrimental to growth in dying trees (Anderegg *et al.*, 2012), whereas warmer conditions may have stimulated growth in surviving trees. This reduced growth and lower climate sensitivity of dying trees could result from a chronic imbalance in their carbon status (e.g. associated with leaf or root dieback) and impaired hydraulic conductance, related to loss of sapwood area over time (Dickman *et al.*, 2015; Pellizzari *et al.*, 2016; Cailleret *et al.*, 2017; Trugman *et al.*, 2018). Norway spruce trees experienced one multiyear drought from 1999 to 2004, while some Scots pine sites were affected by several droughts, including multiyear droughts, during the extended period between 1950 and 2005. Drought-killed Norway spruce and Scots pine trees were less able to utilize summer precipitation than surviving trees (Figs 4 and 5), again perhaps reflecting hydraulic limitations associated with reduced leaf, sapwood, or root area, greater sensitivity of stomatal conductance to atmospheric demand, or differences in rooting depths (Magnani *et al.*, 2002; Jyske *et al.*, 2010; Martinez Del Castillo *et al.*, 2024).

Dying Norway spruce trees in this study were found on rockier and poorly drained, fine-grained soils compared with their surviving counterparts, which may have limited their rooting area and exposed their roots to drier conditions more frequently (Mäkinen *et al.*, 2001; Aakala *et al.*, 2011). Additionally, compared with other species in this study, Norway spruce trees were sampled from a more central part of their geographic range (Mäkinen *et al.*, 2001; Aakala *et al.*, 2011), where droughts were less severe and less frequent. As a result, trees that occur in better microsite conditions and have higher climate sensitivity may recover from drought more effectively. The flashy responses to climate may be less risky and more rewarding for these surviving Norway spruce and Scots pine, as their locations had mean annual precipitation (MAP) that was 1.5 to 2.5 times higher than that of the sites sampled for Engelmann spruce and subalpine fir.

Declining sensitivity (H3) is not consistently related to drought mortality

While 'decline' in vigor or climate sensitivity is a conceptually attractive theory for tree mortality, we found that both drought-surviving and drought-killed trees showed both decreasing ('declining') and increasing ('enhanced') trends in climate sensitivities for multiple seasonal climate variables. Dying subalpine fir showed declining sensitivity to summer precipitation, summer temperature, and winter precipitation, providing support for H3. Unlike other species in this study, the subalpine fir and Engelmann spruce sites represented high-elevation communities in the Colorado Rockies, USA. Recent climate warming in these forest–alpine ecotones has resulted in compounding stressors, such as dramatic changes in snow amount and duration (Siirila-Woodburn *et al.*, 2021), high biotic pressure (Lalande *et al.*, 2020), and unprecedented wildfire events (Higuera *et al.*, 2021), leading to decline (Perret *et al.*, 2023). Consistent with some boreal studies, we found positive trends in the effects of temperature for some species (e.g. Scots pine, Norway spruce, and surviving aspen), highlighting that trees in some sites may benefit from additional warming (Wilmking *et al.*, 2005; Martinez Del Castillo *et al.*, 2024). However, negative trends ('decline') in sensitivity to summer temperature were found for dying and surviving trees (e.g. silver fir and red oak), perhaps suggesting climate change-associated pressures.

Tree responses to climate are also influenced by forest history and disturbances such as fire or thinning (Marqués *et al.*, 2022; Rodman *et al.*, 2024). In the Ozark and Ouachita Mountains in Arkansas, USA, fire suppression has significantly contributed to a decline in climate sensitivity for red oak associated with increased competition (Soucy *et al.*, 2005; Haavik *et al.*, 2011). Our findings indicate that both drought-surviving and drought-killed red oak share similar climate sensitivities, steadily declining in their sensitivities to summer temperature and winter precipitation.

The cessation of fires has led to a marked shift in species establishment and forest succession, which formerly favored oaks in early successional stages, but now shade-tolerant, fire-intolerant species are favored (Soucy *et al.*, 2005). Oaks have a relatively high light requirement; therefore, as forests grew denser in the absence of fire, competition for crucial resources, especially water and light, intensified (Johnson *et al.*, 2002). This increase in competition pressure, combined with the stress of drought conditions, likely resulted in a decline in growth and climate sensitivity of red oak.

Likewise, surviving and dying silver fir trees had similar declining sensitivities to summer temperature. In the Spanish Pyrenees, the observed decline of silver fir may be linked to historical logging practices and drought stress driven by rising temperatures (Camarero *et al.*, 2011). Diameter-limit cutting was the dominant timber harvesting method in this area, affecting primarily fast-growing large trees and thereby allowing smaller, slower-growing trees to persist (Camarero *et al.*, 2017). While the reduction in competition postlogging may have led to temporary increases in biomass, this surge in productivity ultimately proved unsustainable under drought conditions, compromising the carbon balance of remaining trees and leading to a decline in their climate sensitivities.

Negative trends in climate sensitivities were more frequently observed for seasonal temperature effects than for seasonal precipitation effects. This suggests that climate change will likely worsen these negative trends. Additionally, we can expect to see more abrupt changes in growth and possibly increased die-off among trees in the southwestern United States. Trees from the southwestern United States often exhibited divergent trends between drought-killed and surviving trees. Conversely, European tree species showed more consistent trends, with little difference between drought-surviving and dying trees, indicating a greater synchrony with climate. The intense and frequent historical drought events in the arid southwestern United States have likely influenced growth–climate responses. These trends imply that the effects of climate on tree growth may be gradually evolving, and the significant intraspecific differences between drought-surviving and dying trees could reflect important variations in phenotypic plasticity or high-light instability in growth–climate relationships.

Conclusions and future directions

Integrating past studies, we propose a combined framework (flashy-decoupled-declining) for assessing differences in growth among dying and surviving trees, which may be useful for species-specific prediction of future mortality risk. Using this framework, our study shows that climate sensitivity and its role in drought mortality or survival reflect species-specific and regionally specific responses to the environment. Especially in areas such as the southwestern United States, where aridity and drought conditions are extreme and MAP is low, flashy or acquisitive growth strategies can be risky during drought. However, flashy responses to climate may be less risky and more rewarding in areas of northern Europe with relatively higher MAP and lower frequency and intensity of droughts, where climate decoupling can lead to carbon starvation or persistent hydraulic failure. A major finding is that most species had nonstationary climate responses over time (e.g. Peltier & Ogle, 2020), but their growth–climate relationships were inconsistently related to drought-induced mortality. This may reflect ongoing risks of future mortality, even in trees that survived the studies synthesized here.

While the flashy-decoupled-declining framework captures key statistical patterns in growth–climate relationships, future work should more explicitly incorporate plant physiological traits to better understand the mechanisms underlying mortality risk. Species- and site-specific differences in hydraulic vulnerability, leaf area, rooting depth, and carbon allocation strategies likely modulate how trees respond to climate variability and drought stress. Integrating trait data with climate sensitivity models or evaluating correlations between climate sensitivities and traits may enable more predictive, mechanistic assessments of drought mortality risk. This integrated approach would be particularly valuable for forecasting future forest composition under climate change, unifying both climatic drivers and plant resilience strategies.

Acknowledgements

This work was supported by the National Science Foundation under award nos. 2213599 and 1829075. We thank Rohan Boone for the initial data processing.

Competing interests

None declared.

Author contributions

AF and KO designed the study. AF analyzed data and generated the tables, figures and maps with input from DP and KO. AF wrote the first draft of the manuscript. All authors contributed substantially to revisions.

ORCID

Alicia Formanack https://orcid.org/0000-0002-2109-6967
Kiona Ogle https://orcid.org/0000-0002-0652-8397
Drew Peltier https://orcid.org/0000-0003-3271-9055

Data availability

The final dataset and code will be permanently archived and publicly available on GitHub (https://github.com/amf258/Formanacketal_2025) via Zenodo (https://doi.org/10.5281/zenodo.17128082).

References

Aakala T, Kuuluvainen T, Wallenius T, Kauhanen H. 2011. Tree mortality episodes in the intact *Picea abies*-dominated taiga in the Arkhangelsk region of northern European Russia. *Journal of Vegetation Science* **22**: 322–333.

Allen CD, Breshears DD, McDowell NG. 2015. On underestimation of global vulnerability to tree mortality and forest die-off from hotter drought in the Anthropocene. *Ecosphere* **6**: 1–55.

Allen CD, Macalady AK, Chenchouni H, Bachelet D, McDowell N, Vennetier M, Kitzberger T, Rigling A, Breshears DD, Hogg EH *et al.* 2010. A global overview of drought and heat-induced tree mortality reveals emerging climate change risks for forests. *Forest Ecology and Management* **259**: 660–684.

Amoroso MM, Rodríguez-Catón M, Villalba R, Daniels LD. 2017. Forest decline in northern Patagonia: the role of climatic variability. In: Amoroso MM, Daniels LD, Baker PJ, Camarero JJ, eds. *Ecological Studies. Dendroecology*. Cham, Switzerland: Springer International Publishing, 325–342.

Anderegg WRL, Anderegg LDL, Kerr KL, Trugman AT. 2019. Widespread drought-induced tree mortality at dry range edges indicates that climate stress exceeds species' compensating mechanisms. *Global Change Biology* **25**: 3793–3802.

Anderegg WRL, Berry JA, Smith DD, Sperry JS, Anderegg LDL, Field CB. 2012. The roles of hydraulic and carbon stress in a widespread climate-induced forest die-off. *Proceedings of the National Academy of Sciences, USA* **109**: 233–237.

Anderegg WRL, Schwalm C, Biondi F, Camarero JJ, Koch G, Litvak M, Ogle K, Shaw JD, Shevliakova E, Williams AP *et al.* 2015. Pervasive drought legacies in forest ecosystems and their implications for carbon cycle models. *Science* **349**: 528–532.

Anderegg WRL, Trugman AT, Badgley G, Anderson CM, Bartuska A, Ciais P, Cullenward D, Field CB, Freeman J, Goetz SJ *et al.* 2020. Climate-driven risks to the climate mitigation potential of forests. *Science* **368**: eaaz7005.

Baldi P, La Porta N. 2022. Toward the genetic improvement of drought tolerance in conifers: an integrated approach. *Forests* **13**: 2016.

Bigler C, Bräker OU, Bugmann H, Dobbertin M, Rigling A. 2006. Drought as an inciting mortality factor in Scots pine stands of the Valais, Switzerland. *Ecosystems* **9**: 330–343.

Bigler C, Gavin DG, Gunning C, Veblen TT. 2007. Drought induces lagged tree mortality in a subalpine forest in the Rocky Mountains. *Oikos* **116**: 1983–1994.

Bigler C, Gričar J, Bugmann H, Čufar K. 2004. Growth patterns as indicators of impending tree death in silver fir. *Forest Ecology and Management* **199**: 183–190.

Brienen RJW, Caldwell L, Duchesne L, Voelker S, Barichivich J, Baliva M, Ceccantini G, Di Filippo A, Helama S, Locosselli GM *et al.* 2020. Forest carbon sink neutralized by pervasive growth-lifespan trade-offs. *Nature Communications* **11**: 4241.

Brooks SP, Gelman A. 1998. General methods for monitoring convergence of iterative simulations. *Journal of Computational and Graphical Statistics* **7**: 434–455.

Cailleret M, Dakos V, Jansen S, Robert EMR, Aakala T, Amoroso MM, Antos JA, Bigler C, Bugmann H, Caccianaga M *et al.* 2019. Early-warning signals of individual tree mortality based on annual radial growth. *Frontiers in Plant Science* **9**: 1964.

Cailleret M, Jansen S, Robert EMR, Desoto L, Aakala T, Antos JA, Beikircher B, Bigler C, Bugmann H, Caccianiga M *et al.* 2017. A synthesis of radial growth patterns preceding tree mortality. *Global Change Biology* **23**: 1675–1690.

Cailleret M, Nourtier M, Amm A, Durand-Gillmann M, Davi H. 2014. Drought-induced decline and mortality of silver fir differ among three sites in Southern France. *Annals of Forest Science* **71**: 643–657.

Camarero JJ, Bigler C, Linares JC, Gil-Pelegrín E. 2011. Synergistic effects of past historical logging and drought on the decline of Pyrenean silver fir forests. *Forest Ecology and Management* **262**: 759–769.

Camarero JJ, Linares JC, Sangüesa-Barreda G, Sánchez-Salguero R, Gazol A, Navarro-Cerrillo RM, Carreira JA. 2017. The multiple causes of forest decline in Spain: drought, historical logging, competition and biotic stressors. In: Amoroso MM, Daniels LD, Baker PJ, Camarero JJ, eds. *Ecological Studies. Dendroecology*. Cham, Switzerland: Springer International Publishing, 307–323.

Chen G, Tian H, Zhang C, Liu M, Ren W, Zhu W, Chappelka AH, Prior SA, Lockaby GB. 2012. Drought in the Southern United States over the 20th century: variability and its impacts on terrestrial ecosystem productivity and carbon storage. *Climatic Change* **114**: 379–397.

Choat B, Brodribb TJ, Brodersen CR, Duursma RA, López R, Medlyn BE. 2018. Triggers of tree mortality under drought. *Nature* **558**: 531–539.

Crouch CD, Grady AM, Wilhelmi NP, Hofstetter RW, DePinte DE, Waring KM. 2021. Oystershell scale: an emerging invasive threat to aspen in the Southwestern US. *Biological Invasions* **23**: 2893–2912.

DeSoto L, Cailleret M, Sterck F, Jansen S, Kramer K, Robert EMR, Aakala T, Amoroso MM, Bigler C, Camarero JJ *et al.* 2020. Low growth resilience to drought is related to future mortality risk in trees. *Nature Communications* **11**: 545.

Dickman LT, Mcdowell NG, Sevanto S, Pangle RE, Pockman WT. 2015. Carbohydrate dynamics and mortality in a piñon-juniper woodland under three future precipitation scenarios. *Plant, Cell & Environment* **38**: 729–739.

Ford KR, Breckheimer IK, Franklin JF, Freund JA, Kroiss SJ, Larson AJ, Theobald EJ, HilleRisLambers J. 2017. Competition alters tree growth responses to climate at individual and stand scales. *Canadian Journal of Forest Research* **47**: 53–62.

Ford KR, Ettinger AK, Lundquist JD, Raleigh MS, Hille Ris Lambers J. 2013. Spatial heterogeneity in ecologically important climate variables at coarse and fine scales in a high-snow mountain landscape F De Bello, Ed. *PLoS One* **8**: e65008.

Gazol A, Camarero JJ, Vicente-Serrano SM, Sánchez-Salguero R, Gutiérrez E, De Luis M, Sangüesa-Barreda G, Novak K, Rozas V, Tíscar PA *et al.* 2018. Forest resilience to drought varies across biomes. *Global Change Biology* **24**: 2143–2158.

Gazol A, Fajardo A, Camarero JJ. 2023. Contributions of intraspecific variation to drought tolerance in trees. *Current Forestry Reports* **9**: 461–472.

Gea-Izquierdo G, Viguera B, Cabrera M, Cañellas I. 2014. Drought induced decline could portend widespread pine mortality at the xeric ecotone in managed mediterranean pine-oak woodlands. *Forest Ecology and Management* **320**: 70–82.

Gelman A, Carlin JB, Stern HS, Dunson DB, Vehtari A, Rubin DB. 2014. *Bayesian data analysis*. Boca Raton, London; New York, NY, USA: CRC Press, Taylor & Francis Group.

Gelman A, Rubin DB. 1992. Inference from iterative simulation using multiple sequences. *Statistical Science* **7**: 457–472.

Gessler A, Schaub M, McDowell NG. 2017. The role of nutrients in drought-induced tree mortality and recovery. *New Phytologist* **214**: 513–520.

Gillner S, Rüger N, Roloff A, Berger U. 2013. Low relative growth rates predict future mortality of common beech (*Fagus sylvatica* L.). *Forest Ecology and Management* **302**: 372–378.

Haavik LJ, Stahle DW, Stephen FM. 2011. Temporal aspects of *Quercus rubra* decline and relationship to climate in the Ozark and Ouachita Mountains, Arkansas. *Canadian Journal of Forest Research* **41**: 773–781.

Hammond WM, Williams AP, Abatzoglou JT, Adams HD, Klein T, López R, Sáenz-Romero C, Hartmann H, Breshears DD, Allen CD. 2022. Global field observations of tree die-off reveal hotter-drought fingerprint for Earth's forests. *Nature Communications* **13**: 1761.

Harris I, Osborn TJ, Jones P, Lister D. 2020. Version 4 of the CRU TS monthly high-resolution gridded multivariate climate dataset. *Scientific Data* **7**: 109.

Hereş A-M, Martínez-Vilalta J, Claramunt LB. 2012. Growth patterns in relation to drought-induced mortality at two Scots pine (*Pinus sylvestris* L.) sites in NE Iberian Peninsula. *Trees* **26**: 621–630.

Hesse BD, Gebhardt T, Hafner BD, Hikino K, Reitsam A, Gigl M, Dawid C, Häberle K-H, Grams TEE. 2023. Physiological recovery of tree water relations upon drought release—response of mature beech and spruce after five years of recurrent summer drought. *Tree Physiology* **43**: 522–538.

Higuera PE, Shuman BN, Wolf KD. 2021. Rocky Mountain subalpine forests now burning more than any time in recent millennia. *Proceedings of the National Academy of Sciences, USA* **118**: e2103135118.

Huang J, Hammerbacher A, Gershenzon J, Van Dam NM, Sala A, McDowell NG, Chowdhury S, Gleixner G, Trumbore S, Hartmann H. 2021. Storage of carbon reserves in spruce trees is prioritized over growth in the face of carbon limitation. *Proceedings of the National Academy of Sciences, USA* **118**: e2023297118.

Ireland KB, Moore MM, Fulé PZ, Zegler TJ, Keane RE. 2014. Slow lifelong growth predisposes *Populus tremuloides* trees to mortality. *Oecologia* **175**: 847–859.

Johnson PS, Shifley SR, Rogers R. 2002. *The ecology and silviculture of oaks*. Oxon, UK: CABI Publ.

Jyske T, Holtta T, Makinen H, Nojd P, Lumme I, Spiecker H. 2010. The effect of artificially induced drought on radial increment and wood properties of Norway spruce. *Tree Physiology* **30**: 103–115.

Kellner K. 2024. jagsui: A wrapper around 'rjags' to streamline 'JAGS' analyses.

Kolb T, Keefover-Ring K, Burr SJ, Hofstetter R, Gaylord M, Raffa KF. 2019. Drought-mediated changes in tree physiological processes weaken tree defenses to bark beetle attack. *Journal of Chemical Ecology* **45**: 888–900.

Lalande BM, Hughes K, Jacobi WR, Tinkham WT, Reich R, Stewart JE. 2020. Subalpine fir mortality in Colorado is associated with stand density, warming climates and interactions among fungal diseases and the western balsam bark beetle. *Forest Ecology and Management* **466**: 118133.

Leifsson C, Buras A, Rammig A, Zang C. 2023. Changing climate sensitivity of secondary growth following extreme drought events in forest ecosystems: a global analysis. *Environmental Research Letters* **18**: 014021.

Li M-Y, Fang L-D, Duan C-Y, Cao Y, Yin H, Ning Q-R, Hao G-Y. 2020. Greater risk of hydraulic failure due to increased drought threatens pine plantations in Horqin Sandy Land of northern China. *Forest Ecology and Management* **461**: 117980.

Linares JC, Camarero JJ. 2012. Growth patterns and sensitivity to climate predict silver fir decline in the Spanish Pyrenees. *European Journal of Forest Research* **131**: 1001–1012.

Lloyd AH, Duffy PA, Mann DH. 2013. Nonlinear responses of white spruce growth to climate variability in interior Alaska. *Canadian Journal of Forest Research* **43**: 331–343.

Luo Y, McIntire EJB, Boisvenue C, Nikiema PP, Chen HYH. 2020. Climatic change only stimulated growth for trees under weak competition in central boreal forests. *Journal of Ecology* **108**: 36–46.

Magnani F, Grace J, Borghetti M. 2002. Adjustment of tree structure in response to the environment under hydraulic constraints. *Functional Ecology* **16**: 385–393.

Mäkinen H, Nöjd P, Mielikäinen K. 2001. Climatic signal in annual growth variation in damaged and healthy stands of Norway spruce (*Picea abies* (L.) *Karst.*) in southern Finland. *Trees* **15**: 177–185.

Maracahipes L, Carlucci MB, Lenza E, Marimon BS, Marimon BH, Guimarães FAG, Cianciaruso MV. 2018. How to live in contrasting habitats? Acquisitive and conservative strategies emerge at inter- and intraspecific levels in savanna and forest woody plants. *Perspectives in Plant Ecology, Evolution and Systematics* **34**: 17–25.

Marqués L, Peltier DMP, Camarero JJ, Zavala MA, Madrigal-González J, Sangüesa-Barreda G, Ogle K. 2022. Disentangling the legacies of climate and management on tree growth. *Ecosystems* **25**: 215–235.

Martinelli N. 2004. Climate from dendrochronology: latest developments and results. *Global and Planetary Change* **40**: 129–139.

Martinez Del Castillo E, Torbenson MCA, Reinig F, Tejedor E, De Luis M, Esper J. 2024. Contrasting future growth of Norway spruce and Scots pine forests under warming climate. *Global Change Biology* **30**: e17580.

McDowell NG, Sapes G, Pivovaroff A, Adams HD, Allen CD, Anderegg WRL, Arend M, Breshears DD, Brodribb T, Choat B *et al.* 2022. Mechanisms of woody-plant mortality under rising drought, CO_2 and vapour pressure deficit. *Nature Reviews Earth and Environment* **3**: 294–308.

McDowell NG, Williams AP, Xu C, Pockman WT, Dickman LT, Sevanto S, Pangle R, Limousin J, Plaut J, Mackay DS *et al.* 2016. Multi-scale predictions of massive conifer mortality due to chronic temperature rise. *Nature Climate Change* **6**: 295–300.

Meir P, Mencuccini M, Dewar RC. 2015. Drought-related tree mortality: addressing the gaps in understanding and prediction. *New Phytologist* **207**: 28–33.

Minorsky PV. 2003. The decline of sugar maples (*Acer saccharum*). *Plant Physiology* **133**: 441–442.

Nadal-Sala D, Grote R, Birami B, Knüver T, Rehschuh R, Schwarz S, Ruehr NK. 2021. Leaf shedding and non-stomatal limitations of photosynthesis mitigate hydraulic conductance losses in Scots pine saplings during severe drought stress. *Frontiers in Plant Science* **12**: 715127.

Ogle K, Barber JJ, Barron-Gafford GA, Bentley LP, Young JM, Huxman TE, Loik ME, Tissue DT. 2015. Quantifying ecological memory in plant and ecosystem processes. *Ecology Letters* **18**: 221–235.

Ogle K, Whitham TG, Cobb NS. 2000. Tree-ring variation in pinyon predicts likelihood of death following severe drought. *Ecology* **81**: 3237–3243.

Pellizzari E, Camarero JJ, Gazol A, Sangüesa-Barreda G, Carrer M. 2016. Wood anatomy and carbon-isotope discrimination support long-term hydraulic deterioration as a major cause of drought-induced dieback. *Global Change Biology* **22**: 2125–2137.

Peltier DMP, Barber JJ, Ogle K. 2018. Quantifying antecedent climatic drivers of tree growth in the Southwestern US. *Journal of Ecology* **106**: 613–624.

Peltier DMP, Fell M, Ogle K. 2016. Legacy effects of drought in the Southwestern United States: a multi-species synthesis. *Ecological Monographs* **86**: 312–326.

Peltier DMP, Ogle K. 2020. Tree growth sensitivity to climate is temporally variable. *Ecology Letters* **23**: 1561–1572.

Perret DL, Bell DM, Gray AN, Shaw JD, Zald HSJ. 2023. Range-wide population assessments for subalpine fir indicate widespread disturbance-driven decline. *Forest Ecology and Management* **542**: 121128.

Plummer M. 2003. JAGS: a program for analysis of Bayesian graphical models using Gibbs sampling. In: *125.10. Proceedings of the 3rd international workshop on distributed statistical computing*. Vienna, Austria: R Foundation for Statistical Computing, 1–10.

Plummer M. 2008. RJAGS: Bayesian graphical models using MCMC. Version 4–17.

R Core Team. 2022. *R: A language and environment for statistical computing*. Vienna, Austria: R Foundation for Statistical Computing.

Rodman KC, Bradford JB, Formanack AM, Fulé PZ, Huffman DW, Kolb TE, Miller-ter Kuile AT, Normandin DP, Ogle K, Pedersen RJ *et al.* 2024. Restoration treatments enhance tree growth and alter climatic constraints during extreme drought. *Ecological Applications* **35**: e3072.

Sánchez-Salguero R, Camarero JJ, Gutiérrez E, González Rouco F, Gazol A, Sangüesa-Barreda G, Andreu-Hayles L, Linares JC, Seftigen K. 2017. Assessing forest vulnerability to climate warming using a process-based model of tree growth: bad prospects for rear-edges. *Global Change Biology* **23**: 2705–2719.

Sangüesa-Barreda G, Linares JC, Julio CJ. 2013. Drought and mistletoe reduce growth and water-use efficiency of Scots pine. *Forest Ecology and Management* **296**: 64–73.

Schöngart J, Orthmann B, Hennenberg KJ, Porembski S, Worbes M. 2006. Climate–growth relationships of tropical tree species in West Africa and their potential for climate reconstruction. *Global Change Biology* **12**: 1139–1150.

Siirila-Woodburn ER, Rhoades AM, Hatchett BJ, Huning LS, Szinai J, Tague C, Nico PS, Feldman DR, Jones AD, Collins WD *et al.* 2021. A low-to-no snow future and its impacts on water resources in the western United States. *Nature Reviews Earth and Environment* **2**: 800–819.

Smith IA, Dearborn VK, Hutyra LR. 2019. Live fast, die young: accelerated growth, mortality, and turnover in street trees. *PLoS One* **14**: e0215846.

Soucy RD, Heitzman E, Spetich MA. 2005. The establishment and development of oak forests in the Ozark Mountains of Arkansas. *Canadian Journal of Forest Research* **35**: 1790–1797.

Stokes MA. 1996. *An introduction to tree-ring dating*. Tucson, AZ, USA: University of Arizona Press.

Swain DL, Prein AF, Abatzoglou JT, Albano CM, Brunner M, Diffenbaugh NS, Singh D, Skinner CB, Touma D. 2025. Hydroclimate volatility on a warming Earth. *Nature Reviews Earth and Environment* **6**: 35–50.

Tipton J, Hooten M, Pederson N, Tingley M, Bishop D. 2016. Reconstruction of late Holocene climate based on tree growth and mechanistic hierarchical models. *Environmetrics* **27**: 42–54.

Tomasella M, Häberle K-H, Nardini A, Hesse B, Machlet A, Matyssek R. 2017. Post-drought hydraulic recovery is accompanied by non-structural carbohydrate depletion in the stem wood of Norway spruce saplings. *Scientific Reports* **7**: 14308.

Trugman AT, Anderegg LDL, Anderegg WRL, Das AJ, Stephenson NL. 2021. Why is tree drought mortality so hard to predict? *Trends in Ecology & Evolution* **36**: 520–532.

Trugman AT, Detto M, Bartlett MK, Medvigy D, Anderegg WRL, Schwalm C, Schaffer B, Pacala SW. 2018. Tree carbon allocation explains forest drought-kill and recovery patterns. *Ecology Letters* **21**: 1552–1560.

Umaña MN, Salgado-Negret B, Norden N, Salinas V, Garzón F, Medina SP, Rodríguez-M GM, López-Camacho R, Castaño-Naranjo A, Cuadros H *et al.* 2023. Upscaling the effect of traits in response to drought: the relative importance of safety–efficiency and acquisitive–conservation functional axes. *Ecology Letters* **26**: 2098–2109.

Van Mantgem PJ, Stephenson NL, Byrne JC, Daniels LD, Franklin JF, Fulé PZ, Harmon ME, Larson AJ, Smith JM, Taylor AH *et al.* 2009. Widespread increase of tree mortality rates in the Western United States. *Science* **323**: 521–524.

Voelker SL, Muzika R-M, Guyette RP. 2008. Individual tree and stand level influences on the growth, vigor, and decline of red oaks in the Ozarks. *Forest Science* **54**: 8–20.

Willi Y, Van Buskirk J. 2022. A review on trade-offs at the warm and cold ends of geographical distributions. *Philosophical Transactions of the Royal Society, B: Biological Sciences* **377**: 20210022.

Williams AP, Cook BI, Smerdon JE. 2022. Rapid intensification of the emerging southwestern North American megadrought in 2020–2021. *Nature Climate Change* **12**: 232–234.

Williams AP, Cook ER, Smerdon JE, Cook BI, Abatzoglou JT, Bolles K, Baek SH, Badger AM, Livneh B. 2020. Large contribution from anthropogenic warming to an emerging North American megadrought. *Science* **368**: 314–318.

Wilmking M, D'Arrigo R, Jacoby GC, Juday GP. 2005. Increased temperature sensitivity and divergent growth trends in circumpolar boreal forests. *Geophysical Research Letters* **32**: 2005GL023331.

Wilmking M, Van Der Maaten-Theunissen M, Van Der Maaten E, Scharnweber T, Buras A, Biermann C, Gurskaya M, Hallinger M, Lange J, Shetti R *et al.* 2020. Global assessment of relationships between climate and tree growth. *Global Change Biology* **26**: 3212–3220.

Wright SJ, Kitajima K, Kraft NJB, Reich PB, Wright IJ, Bunker DE, Condit R, Dalling JW, Davies SJ, Díaz S *et al.* 2010. Functional traits and the growth–mortality trade-off in tropical trees. *Ecology* **91**: 3664–3674.

Zeng Z, Wu W, Li Y, Huang C, Zhang X, Peñuelas J, Zhang Y, Gentine P, Li Z, Wang X *et al.* 2023. Increasing meteorological drought under climate change reduces terrestrial ecosystem productivity and carbon storage. *One Earth* **6**: 1326–1339.

Zhang Y, Keenan TF, Zhou S. 2021. Exacerbated drought impacts on global ecosystems due to structural overshoot. *Nature Ecology & Evolution* **5**: 1490–1498.

Supporting Information

Additional Supporting Information may be found online in the Supporting Information section at the end of the article.

Fig. S1 Scatter plots of predicted vs observed ring width in millimeters for drought-killed trees for the seven study species.

Fig. S2 Scatter plots of predicted vs observed ring width in millimeters for drought-surviving trees for the seven study species.

Fig. S3 Posterior estimates of the climate effects by status and species.

Fig. S4 Realized climate sensitivities for drought-surviving and drought-killed trees for *Abies alba* (silver fir) associated with each seasonal climate variable: winter precipitation, winter temperature, summer precipitation, and summer temperature.

Fig. S5 Realized climate sensitivities for drought-surviving and drought-killed trees for *Abies lasiocarpa* (subalpine fir) associated with each seasonal climate variable: winter precipitation, winter temperature, summer precipitation, and summer temperature.

Fig. S6 Realized climate sensitivities for drought-surviving and drought-killed trees for *Picea abies* (Norway spruce) associated with each seasonal climate variable: winter precipitation, winter temperature, summer precipitation, and summer temperature.

Fig. S7 Realized climate sensitivities for drought-surviving and drought-killed trees for Picea engelmannii (Engelmann spruce) associated with each seasonal climate variable: winter precipitation, winter temperature, summer precipitation, and summer temperature.

Fig. S8 Realized climate sensitivities for drought-surviving and drought-killed trees for *Pinus sylvestris* (Scots pine) associated with each seasonal climate variable: winter precipitation, winter temperature, summer precipitation, and summer temperature.

Fig. S9 Realized climate sensitivities for drought-surviving and drought-killed (rust-colored lines and shading) trees for *Populus tremuloides* (quaking aspen) associated with each seasonal climate variable: winter precipitation, winter temperature, summer precipitation, and summer temperature.

Fig. S10 Realized climate sensitivities for drought-surviving and drought-killed trees for *Quercus rubra* (red oak) associated with each seasonal climate variable: winter precipitation, winter temperature, summer precipitation, and summer temperature.

Please note: Wiley is not responsible for the content or functionality of any Supporting Information supplied by the authors. Any queries (other than missing material) should be directed to the *New Phytologist* Central Office.